Quantum-Chemical Study of the Effect of Triethylaluminum on the Chain-End Structure and Tacticity of Poly(*N*,*N*-dimethylacrylamide) with Lithium Counterion in THF

Alexander V. Yakimansky† and Axel H. E. Müller*

Makromolekulare Chemie II and Bayreuther Zentrum für Kolloide und Grenzflächen, Universität Bayreuth, D-95440 Bayreuth, Germany

Received February 22, 2006; Revised Manuscript Received March 27, 2006

ABSTRACT: Quantum-chemical DFT calculations of the structures and relative stabilities of poly(*N*,*N*-dimethylacrylamide) anionic living chain ends with lithium counterion and their aggregates in THF, both in the absence and in the presence of the Lewis acid (LA) triethylaluminum (Et_3Al), were performed. LA-coordinated, solvated unimers are the most stable species in the presence of Et_3Al, whereas unimers and dimers coexist in the absence of LA. In all cases coordination of Li^+ to the penultimate and/or antepenultimate amide unit of the chain end is energetically unfavorable. In the presence of LA, the triads with ultimate *r*-dyads are systematically more favorable than those with ultimate *m*-dyads. This correlates with the observed formation of heterotactic polymers in the presence of Et_3Al. It was shown that the polymerization kinetics is determined by the competition for complexation with Et_3Al between solvent, monomer, and carbonyl groups of predominantly heterotactic polymer chains (in the presence of Et_3Al). Complex formation between LA and heterotactic in-chain triads is much less favorable than those between LA and either THF or monomer molecules. Therefore, the fraction of monomer activated by the LA complexation increases with increasing conversion, leading to an increase of the observed polymerization rate.

Introduction

Poly(*N*,*N*-dimethylacrylamide) (PDMAAm) and its copolymers are important materials in such applications as peptide separation,[1] DNA sequencing separations by capillary electrophoresis,[2,3] tissue engineering,[4] slow drug release,[5] solubilization of fullerene into water,[6] oil recovery,[7] etc. Therefore, it is important to control structural and molecular weight characteristics of PDMAAm during its synthesis, the most reliable approach being the living anionic polymerization of *N*,*N*-dimethylacrylamide (DMAAm). The polymerization of DMAAm by organolithium initiators in both hydrocarbon media[8] and THF[9−13] is not well controlled due to formation of insoluble highly crystalline polymers with predominantly isotactic microstructure.[10−12,14−17]

Recently, to control the polymerization of DMAAm, new effective anionic initiating systems were developed, consisting of organometallic compounds of group I and II metals modified by such Lewis acids (LA) as Et_3B,[10] Et_2Zn,[10−12,14,15] and Et_3Al.[16,17] It has been found that in the presence of Lewis acids soluble and highly syndiotactic[10−12] or heterotactic[10−12,16,17] polymers are formed with predictable molecular weight and narrow molecular weight distribution,[10−12,14,15] even at 30 °C.[10]

The anionic polymerization of *N*,*N*-diethylacrylamide (DEAAm) is controlled by Lewis acids in a similar way.[11,12] The corresponding polymers show LCST (lower critical solution temperature) behavior in water close to body temperature, which makes them very attractive materials for biological and medical applications.[18−20] Recent kinetic data on the polymerization of DEAAm in THF in the presence of Et_3Al indicate a very complex reaction mechanism.[21,22] It is reasonable to assume that the mechanisms for the two dialkylacrylamide monomers do not differ substantially.

Although a coordination of Lewis acids to the propagating amidoenolate anions is obvious in these processes,[10−12] available experimental data are not sufficient to understand the structures of active chain ends and their effect on kinetics and tacticity in detail. In this paper, we present quantum-chemical density functional theory data on the structure and relative stabilities of different forms of PDMAAm-Li chain end fragments in THF both in the presence and in the absence of Et_3Al. The effect of the Lewis acid on the relative stabilities of chain end triadic sequences with different tacticities is analyzed.

Methods of Computation

All density functional theory (DFT) geometry optimizations were performed using the TURBOMOLE program.[23] A BP86[24−26] gradient corrected functional in the RI formalism[27−29] has been used throughout for the geometry optimizations. The energetics has been checked by single-point calculations with a B3LYP functional.[30,31] The numerical integration scheme using a "m3" grid has been described in ref 32. For the fitting of the Coulomb potential within the RI formalism, Ahlrichs auxiliary basis sets[28,33] have been used. The geometry optimizations have been carried out using a split-valence (SV) basis set augmented with polarization functions for non-hydrogen atoms. This basis (which is comparable to a 6-31G*) is referred to as SVP.[34]

In some cases, ^{13}C NMR shifts on C^{α} atoms of enolate fragments were calculated by the GIAO-SCF method[35] implemented into the TURBOMOLE program. For the NMR shift calculations, Hartree−Fock (HF) molecular orbitals were calculated at the BP86/SVP-optimized geometries with the TZVP basis set of triple-ζ quality for the valence shells with polarization functions for non-hydrogen atoms.[36,37]

For all considered structures of the type $(RLi)_n(THF)_x(LA)_y$ ($n = 1, 2$; $x = 1-4$; $y = 0-2$), the values of the averaged energy per one model chain end, RLi, $\bar{E}[(RLi)_n(THF)_x(LA)_y]$, was calculated as a comparable stability parameter:

$$\bar{E}[(RLi)_n(THF)_x(LA)_y] = \frac{E[(RLi)_n(THF)_x(LA)_y] - (x-y)E(THF) - yE(LA\cdot THF)}{n} \quad (1)$$

† Permanent address: Institute of Macromolecular Compounds of the Russian Academy of Sciences, Bolshoi prospect 31, 199004 St. Petersburg, Russia.

* Corresponding author. E-mail: axel.mueller@uni-bayreuth.de.

10.1021/ma060385r CCC: $33.50
Published on Web 05/13/2006

Table 1. Calculated Complex Formation Energies, ΔE, and Basis Set Superposition Errors, E_{BSSE}, for the Reaction between Aluminum Hydride and Dimethyl Ether

level of theory	ΔE, kJ/mol	E_{BSSE}, kJ/mol	$\Delta E + E_{BSSE}$, kJ/mol
BP86/SVP//BP86/SVP	−96.7	15.9	−80.8
B3LYP/TZVP//BP86/SVP	−85.4	4.1	−81.3
MP2/TZVPP//BP86/SVP	−103.9	6.7	−97.2

where $E[(RLi)_n(THF)_x(LA)_y]$ denotes the minimized total energy of the particular structure and E(THF) and E(LA·THF) are minimized total energies of an isolated THF molecule and its complex with a given LA molecule, respectively. Relative stabilities of different structures are characterized by their $\Delta\bar{E}$ values with respect to the most stable structure for which $\Delta\bar{E} = 0$. The calculated E, $\bar{E}$, and $\Delta\bar{E}$ values for all structures are presented in Tables 2 and 3. For these systems, several possible backbone and side-group conformations, as well as those of alkyl groups of Lewis acids, were optimized, and the structures with the minimal total energy values, E, were selected.

For the most important of the considered complexes, basis set superposition errors (BSSE) were calculated by the counterpoise method, correcting for an artificial overestimation of a complex stability due to the fact that the whole supermolecular basis set is used to describe the "internal" energy of molecules, forming the complex.[38,39]

In our previous papers, relative stabilities of different forms of anionic chain ends were successfully described at the B3LYP/TZVP//BP86/SVP level of theory.[40−42] In the present work it seemed reasonable first to verify the performance of both BP86/SVP//BP86/SVP and B3LYP/TZVP//BP86/SVP levels for the complexes between R_3Al and ethers, comparing their predictions for the complex formation energies with those obtained at a higher level of theory. For the verification, the MP2/TZVPP//BP86/SVP level of theory was chosen which includes MP2 single-point energy calculations with the TZVPP basis set, containing three sets of polarizations functions for main-group elements.[43]

Because of the very large size of the TZVPP basis set, the MP2 calculations were only possible for the H_3Al−dimethyl ether system. The results (Table 1) show that both BP86/SVP//BP86/SVP and B3LYP/TZVP//BP86/SVP underestimate the complex formation energy, ΔE, compared to that calculated at the MP2/TZVPP//BP86/SVP level. It should be noted that ca. 19 kJ/mol difference in the ΔE values calculated at the B3LYP/TZVP//BP86/SVP and MP2/TZVPP//BP86/SVP levels is very close to the difference of ca. 16 kJ/mol between B3LYP and MP2 predictions for the system Et_3Al−dimethyl ether.[44] However, with BSSE taken into account, the results at the BP86/SVP//BP86/SVP and B3LYP/TZVP//BP86/SVP levels are almost identical. Therefore, the data obtained at both levels of theory are presented below.

Results and Discussion

Lewis Acid-Free Chain-End Structures. Scheme 1 and Figure 1 show the optimized structures of the aggregated and nonaggregated THF-solvated model of the PDMAAm-Li chain end, the enolate of *N*,*N*-dimethylpropionamide, DMPAm-Li, in the absence of LA.

As seen from the data presented in Table 2, in the absence of Et_3Al, the most stable structure is the dimer, $(DMPAm\text{-}Li)_2$·4THF (Figure 1a). It is ca. 24 kJ/mol more stable than the nonaggregated model chain end, $(DMPAm{-}Li)_1$·3THF (Figure 1b). According to the calculation data, the C^α atom ^{13}C NMR signal of the dimer, $(DMPAm\text{-}Li)_2$·4THF, is shifted ca. 4.5 ppm downfield with respect to that of the $(DMPAm\text{-}Li)_1$·3THF structure (Table 2). This is due to a considerably lower electron density on the C^α atom of the former as compared to that of the latter, correlating with commonly recognized much lower propagation rate constants of aggregated chain ends as compared to that nonaggregated species.[45]

Chain-End Structures in the Presence of LA. The data presented in Table 2 show that Et_3Al induces an efficient deaggregation of the $(DMPAm\text{-}Li)_2$·4THF dimers into the most stable nonaggregated species $(DMPAm\text{-}Li)_1$·3THF·Et_3Al ($\Delta\bar{E} = -20.9$ and −17.6 kJ/mol at the BP86/SVP//BP86/SVP and B3LYP/TZVP//BP86/SVP levels of theory, respectively), in which the Et_3Al is coordinated to the enolate oxygen atom (Figure 1c). In contrast, it was found earlier that the site of preferential complexation of Et_3Al with the lithium enolate of methyl isobutyrate (in a nonpolar solvent) is its ether oxygen rather than enolate oxygen atom.[46]

The BSSE-corrected reaction energies for the processes 2 and 3

$$^1/_2[(DMPAm\text{-}Li)_2\cdot 4THF] + THF \rightleftharpoons (DMPAm\text{-}Li)_1\cdot 3THF \quad (2)$$

$$(DMPAm\text{-}Li)_1\cdot 3THF + THF\cdot Et_3Al \rightleftharpoons (DMPAm\text{-}Li)_1\cdot 3THF\cdot Et_3Al + THF \quad (3)$$

could be calculated from the data of Table 2 as

$$\Delta E(2) = \Delta\bar{E}((DMPAm\text{-}Li)_1\cdot 3THF) + \bar{E}_{BSSE}((DMPAm\text{-}Li)_1\cdot 3THF) - \Delta\bar{E}((DMPAm\text{-}Li)_2\cdot 4THF) - \bar{E}_{BSSE}((DMPAm\text{-}Li)_2\cdot 4THF)$$

$$\Delta E(3) = \Delta\bar{E}((DMPAm\text{-}Li)_1\cdot 3THF\cdot Et_3Al) + \bar{E}_{BSSE}((DMPAm\text{-}Li)_1\cdot 3THF\cdot Et_3Al) - \Delta\bar{E}((DMPAm\text{-}Li)_1\cdot 3THF) - \bar{E}_{BSSE}(THF\cdot Et_3Al)$$

(in reaction 3, $(DMPAm\text{-}Li)_1$·3THF is considered as a single molecule for which $\bar{E}_{BSSE} = 0$). This gives $\Delta E(2) = 26.5$ and 24.2 kJ/mol and $\Delta E(3) = -34.1$ and −38.8 kJ/mol at the BP86/SVP//BP86/SVP and B3LYP/TZVP//BP86/SVP levels of theory. Then, for the sum of processes 2 and 3

$$^1/_2[(DMPAm\text{-}Li)_2\cdot 4THF] + THF\cdot Et_3Al \rightleftharpoons (DMPAm\text{-}Li)_1\cdot 3THF\cdot Et_3Al \quad (4)$$

the BSSE-corrected reaction energy $\Delta E(4) = \Delta E(2) + \Delta E(3) = -7.6$ and −14.6 kJ/mol at the BP86/SVP//BP86/SVP and B3LYP/TZVP//BP86/SVP levels.

It is important to analyze the reasons for the fact that the apparent rate constant of DEAAm polymerization in the presence of Et_3Al increases with conversion, i.e., with decreasing actual monomer concentration [DEAAm], the apparent rate constant at high conversion not depending on the initial monomer concentration, $[DEAAm]_0$.[21,22] On the basis of the experimental data, an "activated monomer" mechanism was suggested. According to this mechanism, the monomer complexed with the Lewis acid is much more active in propagation than the free monomer. Neglecting for the moment the complexation of Et_3Al to in-chain carbonyl groups, the fraction, α, of the activated monomer could be estimated from the following equilibrium:[21]

$$THF\cdot Et_3Al + DEAAm \rightleftharpoons DEAAm\cdot Et_3Al + THF \quad (5)$$

Table 2. Relative Stabilities, $\Delta\bar{E}$, and Basis Set Superposition Errors per One DMPAm-Li or Et_3Al Fragment, $\bar{E}_{BSSE}$, Calculated at the BP86/SVP//BP86/SVP and B3LYP/TZVP//BP86/SVP (Marked Bold) Levels of Theory, and ^{13}C NMR Shifts for C^{α} Atoms for Different Complexes and/or Aggregates of Chain-End Units, DMPAm-Li

structure	Fig	C^{α} atom ^{13}C NMR shift, ppm	$\Delta\bar{E}$, kJ/mol	BSSE for AB complexes A	B	$\bar{E}_{BSSE}$, kJ/mol
Et_3Al			76.5			
			65.8			
$(Et_3Al)_2$			50.1	Et_3Al	Et_3Al	7.6
			56.7			**1.7**
Et_3Al·THF			0	Et_3Al	THF	20.6
			0			**4.2**
Et_3Al·DMAAm			−7.6	Et_3Al	DMAAm	19.9
			−6.2			**3.4**
$(DMPAm\text{-}Li)_2$·4THF	1a	66.9	0	$(DMPAm\text{-}Li)_1$·2THF	$(DMPAm\text{-}Li)_1$·2THF	20.0
			0			**4.4**
$(DMPAm\text{-}Li)_1$·3THF	1b	62.3	23.0	$(DMPAm\text{-}Li)_1$·2THF	THF	23.5
			23.9			**4.7**
$(DMPAm\text{-}Li)_1$·3THF·Et_3Al	1c	78.6	−20.9	Et_3Al	$(DMPAm\text{-}Li)_1$·3THF	30.4
			−17.4			**6.7**
iso-trimer·Et_3Al	2a		9.6	Et_3Al	iso-trimer	22.6
			7.8			**4.1**
hetero-trimer·Et_3Al	2b		−3.4	Et_3Al	hetero-trimer	23.1
			−1.1			**3.9**
syndio-trimer·Et_3Al	2c		−14.2	Et_3Al	syndio-trimer	22.6
			−9.2			**3.8**

Table 3. Relative Stabilities, $\Delta\bar{E}$, and Basis Set Superposition Errors per One Triadic Chain-End Fragment, $\bar{E}_{BSSE}$, Calculated at the BP86/SVP//BP86/SVP and B3LYP/TZVP//BP86/SVP (Marked Bold) Levels of Theory, for Different Triadic Models of PDMAAm-Li Chain Ends

structure	Fig	coordination of PU to Li^+	coordination of APU to Li^+	$\Delta\bar{E}$, kJ/mol	BSSE for AB complexes A	B	$\bar{E}_{BSSE}$, kJ/mol
$(\sim mx)_1$·3THF	3a			0	$(\sim mx)_1$·2THF	THF	21.9
				0			**4.7**
$(\sim rx)_1$·3THF	3b			5.4	$(\sim rx)_1$·2THF	THF	22.4
				3.8			**4.7**
$(\sim mx)_1$·2THF		yes		18.8			
				15.1			
$(\sim rx)_1$·2THF		yes		18.8			
				17.6			
$(\sim mx)_1$·2THF			yes	24.3			
				23.4			
$(\sim rx)_1$·2THF			yes	33.0			
				29.3			
$(\sim mx)_1$·THF		yes	yes	61.9			
$(\sim rx)_1$·THF		yes	yes	59.8			
$(\sim mx)_2$·4THF	4a			11.3	$(\sim mx)_1$·2THF	$(\sim mx)_1$·2THF	23.4
				10.0			
$(\sim rx)_2$·4THF	4b			4.2	$(\sim rx)_1$·2THF	$(\sim rx)_1$·2THF	22.5
				1.3			
$(mx)_1$·$(rx)_1$·4THF				8.1	$(\sim mx)_1$·2THF	$(\sim rx)_1$·2THF	23.2
$(\sim mm)_1$·3THF·Et_3Al	5a			−12.6	$(\sim mm)_1$·3THF	Et_3Al	30.0
				−12.1			**6.6**
$(\sim mr)_1$·3THF·Et_3Al	5b			−27.6	$(\sim mr)_1$·3THF	Et_3Al	32.4
				−27.3			**7.1**
$(\sim rm)_1$·3THF·Et_3Al	5c			−14.2	$(\sim rm)_1$·3THF	Et_3Al	30.1
				−11.8			**6.5**
$(\sim rr)_1$·3THF·Et_3Al	5d			−23.9	$(\sim rr)_1$·3THF	Et_3Al	32.7
				−20.9			**7.0**

Scheme 1. Unimer and Dimer of the Model Compound, DMPAm-Li

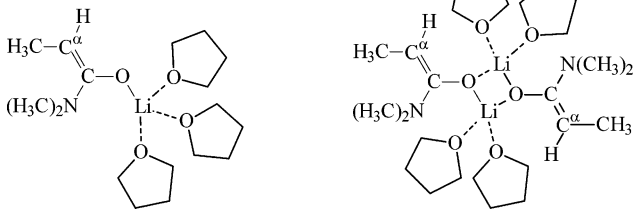

It was shown that the [DEAAm] dependence of α closely mimics that of the apparent polymerization rate constant, the best fitting being obtained at the free energy value of −10.5 kJ/mol for reaction 5.[21] The BSSE-corrected reaction energy for process 5 could be estimated (having replaced DMAAm for DEAAm, Table 2) as $\Delta E(5) = \Delta\bar{E}(DMAAm{\cdot}Et_3Al) + \bar{E}_{BSSE}(DMAAm{\cdot}Et_3Al) - \Delta\bar{E}(THF{\cdot}Et_3Al) - \bar{E}_{BSSE}(THF{\cdot}Et_3Al) = -8.3$ and −7.0 kJ/mol at the BP86/SVP//BP86/SVP and B3LYP/TZVP//BP86/SVP levels, which is in very good agreement with the above-presented experimental estimation. (One could expect that the entropic contribution to the free energy for reaction 5 should be small.)

To compare the energies of complex formation between Et_3Al and in-chain carbonyl groups with that between Et_3Al and the monomer, we calculated iso-, hetero-, and syndio-trimers of PDMAAm chains and their complexes with Et_3Al (Figure 2):

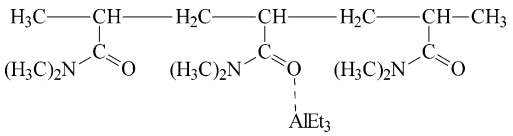

The backbone conformations for these trimeric models were

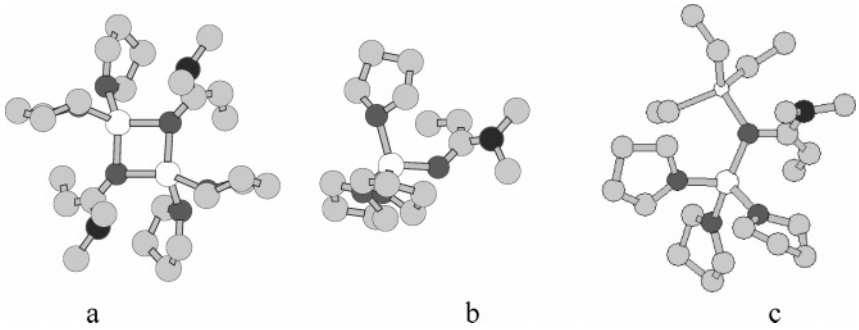

Figure 1. DFT-optimized structures of $(DMPAm\text{-}Li)_2 \cdot 4THF$ (a), $(DMPAm\text{-}Li)_1 \cdot 3THF$ (b), and $(DMPAm\text{-}Li)_1 \cdot 3THF \cdot Et_3Al$ (c). Carbons are shown as light gray spheres, oxygens in dark gray, nitrogens in black, and lithiums in white. Aluminum is shown as a smaller white circle. Hydrogens are not shown.

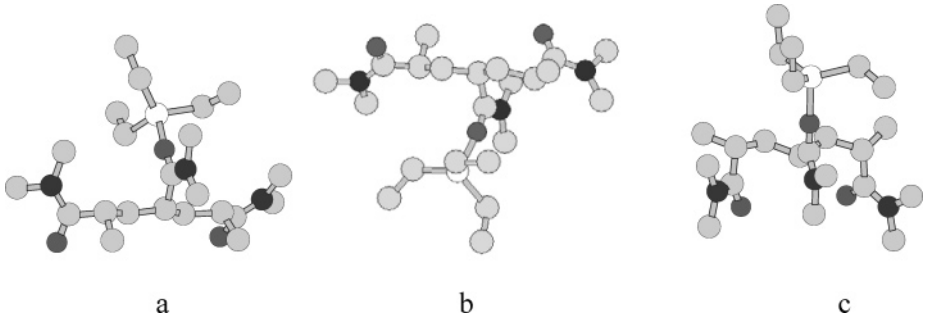

Figure 2. DFT-optimized structures of iso- (a), hetero- (b), and syndiotactic (c) trimeric models of PDMAAm chain fragments, coordinated with Et_3Al. Carbons are shown as light gray spheres, oxygens in dark gray, nitrogens in black, and aluminum in white. Hydrogens are not shown.

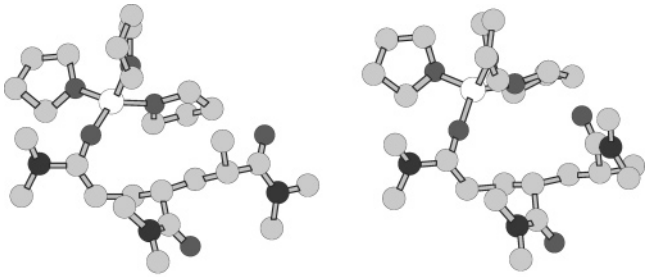

Figure 3. DFT-optimized structures of $(\sim mx)_1 \cdot 3THF$ (a) and $(\sim rx)_1 \cdot 3THF$ (b). Carbons are shown as light gray spheres, oxygens in dark gray, nitrogens in black, and lithiums in white. Hydrogens are not shown.

chosen in a way to retain the most energetically favorable trans-arrangements of backbone torsion angles, unless it was necessary to change some torsion angles to gauche arrangement in order to minimize the mutual repulsion of the bulky neighboring dimethylamido groups. Conformations of side chains were also varied, and optimum conformations were selected.

As seen from Table 2, the calculated complexation energy strongly depends on tacticity, being the highest (the least favorable) for the isotactic (*mm*) trimer and the lowest (the most favorable) for the syndiotactic (*rr*) trimer. However, the complexation energy for the heterotactic (*mr*) trimer is mostly relevant to the experimental situation because polymers formed in the presence of Et_3Al are strongly heterotactic.[21,22] The BSSE-corrected reaction energy for the complex formation

$$\text{hetero-trimer} + \text{THF} \cdot Et_3Al \rightleftharpoons \text{hetero-trimer} \cdot Et_3Al + \text{THF} \quad (6)$$

can be calculated as $\Delta E(6) = \Delta\bar{E}(\text{hetero-trimer} \cdot Et_3Al) + \bar{E}_{BSSE}(\text{hetero-trimer} \cdot Et_3Al) - \bar{E}_{BSSE}(\text{THF} \cdot Et_3Al) = -0.9$ and -1.4 kJ/mol at the BP86/SVP//BP86/SVP and B3LYP/TZVP//BP86/SVP levels; i.e., reaction 6 is much less exothermic (if to any extent) than reaction 5.

It should also be noted that, unlike monomer molecules, all in-chain carbonyl groups cannot be simultaneously LA-complexed due to steric hindrances, leading to a strong neighboring group effect.[47]

LA-Free Triad Chain-End Structures. Scheme 2 shows two-dimensional diagrams of the different calculated triadic models consisting of ultimate (U), penultimate (PU), and antepenultimate (APU) units. Four different structural types of the triadic models, with and without PU unit coordination and/or APU unit coordination to the Li^+ counterion, were analyzed. It should be noted that the intramolecular coordination of either PU or APU unit is accompanied by the decrease in the number of externally solvating THF molecules (Table 3) because the coordination number for Li^+ cations is 4.

The DMAAm monomer attack on the chain end is supposed to occur on the cation side (prochirality concept).[48] However, in the absence of Lewis acids, it was impossible to assign a meso (*m*) or racemic (*r*) structure to the ultimate dyads, i.e., those composed of PU and U units, because in these structures the Li^+ cation is situated nearly on the line of the C−O bond (bond angle C−O−Li ≅ 150°). Therefore, for such structures, having almost no prochirality, ultimate dyads are defined in Table 3 as *x*-dyads.

It is seen from Table 3 that in the absence of Lewis acids the most stable nonassociated triadic structures are THF-solvated *mx*- and *rx*-triads, $(\sim mx)_1 \cdot 3THF$ and $(\sim rx)_1 \cdot 3THF$, in which neither a PU nor an APU unit is coordinated to the terminal Li^+ cation. All the structures with at least one of these coordination types have much higher $\Delta\bar{E}$ values (see Table 3) and, therefore, are disregarded for the analysis of predominant microtacticities in the presence of Et_3Al.

According to the data of Table 3, the structures $(\sim mx)_1 \cdot 3THF$ (Figure 3a) and $(\sim rx)_1 \cdot 3THF$ (Figure 3b) have comparable stabilities, although the former has somewhat lower $\Delta\bar{E}$ value than the latter. However, as seen from Table 3, *rx*-triads form more stable dimeric aggregates, $(\sim rx)_2 \cdot 4THF$ (Figure 4b, $\Delta\bar{E}$

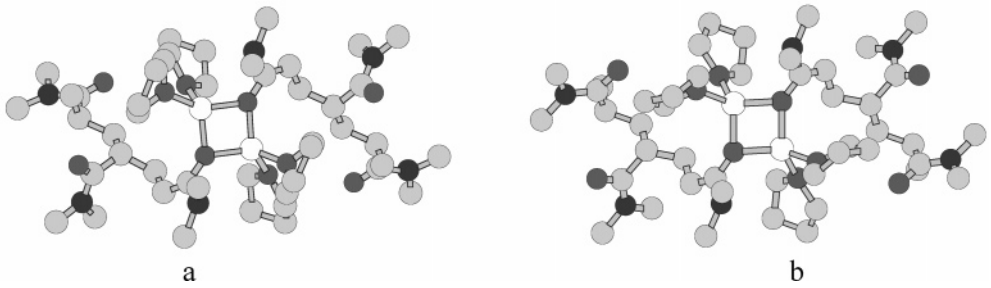

Figure 4. DFT-optimized structures of $(\sim mx)_2$·4THF (a) and $(\sim rx)_2$·4THF (b). Carbons are shown as light gray spheres, oxygens in dark gray, nitrogens in black, and lithiums in white. Hydrogens are not shown.

Scheme 2. Possible Intramolecular Coordinations in Nonassociated Chain Ends (THF Molecules Omitted)

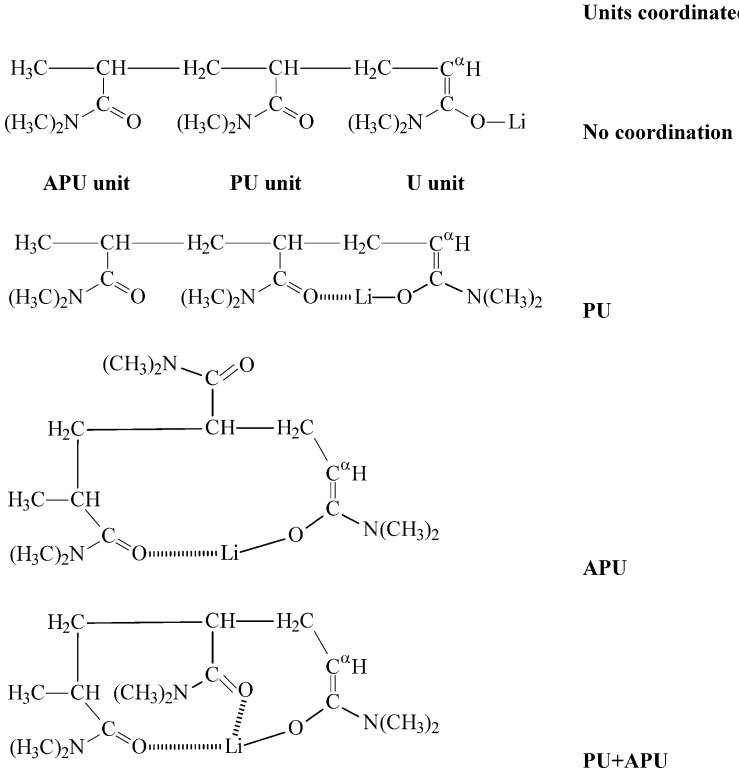

$= 1.3$ kJ/mol at the B3LYP/TZVP//BP86/SVP level of theory), compared to the aggregates of *mx*-triads, $(\sim mx)_2$·4THF (Figure 4a, $\Delta\bar{E} = 10.0$ kJ/mol at the B3LYP/TZVP//BP86/SVP level of theory). Even although there is a certain entropy gain on aggregation (two unimeric chain ends, each being solvated by three THF molecules, react to form a dimeric aggregate, eliminating two THF molecules), these data show that at typical chain end concentrations ($[P^*]_0 \sim 10^{-3}$ M) $K_{ass.} < 1$, and the contribution of aggregates is negligible ($K_{ass.}[P^*]_0 \sim 0.1\%$).

Triad Chain-End Structures in the Presence of LA. Coordination of a Lewis acid to the enolate oxygen atom of the $(\sim mx)_1$·3THF and $(\sim rx)_1$·3THF structures pushes the Li^+ counterion solvated with three THF molecules to the opposite side of the enolate C═C−O plane, making the structure sufficiently prochiral to determine the sense of the ultimate prochiral dyad. Scheme 3 shows a two-dimensional diagram of the corresponding structures.

Penultimate dyads, i.e., those between APU and PU units, are defined as *m*-dyads if the two asymmetric carbon atoms of the APU and PU units have the same optical configuration and as *r*-dyads in the opposite case (Table 3).

Experimental data on DEAAm polymerization kinetics in the presence of Et_3Al demonstrated the decrease of the measured

Scheme 3. LA Coordinated Triads of Chain Ends

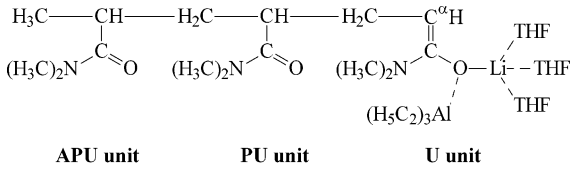

polymerization rate constant with increasing $[Et_3Al]$.[21,22] It was explained by a shift of a fast dynamic equilibrium between active LA-free and dormant LA-complexed chain ends toward the latter ones which progresses with the increase in $[Et_3Al]$:[21,22]

$$(\sim xy)\cdot 3\mathrm{THF} + \mathrm{Et_3Al}\cdot\mathrm{THF} \rightleftharpoons (\sim xy)\cdot 3\mathrm{THF}\cdot\mathrm{Et_3Al} + \mathrm{THF} \quad (7)$$

($x, y = m$ or r). This explanation would only be possible if reaction 7 is not too exothermic because otherwise all chain ends would be LA-complexed already at a quite low $[Et_3Al]$. The BSSE-corrected reaction energies for process 7 are $E_{xy}(7) = \Delta\bar{E}((\sim xy)\cdot 3\mathrm{THF}\cdot\mathrm{Et_3Al}) + \bar{E}_{\mathrm{BSSE}}((\sim xy)\cdot 3\mathrm{THF}\cdot\mathrm{Et_3Al}) - \Delta\bar{E}((\sim xy)\cdot 3\mathrm{THF}) - \bar{E}_{\mathrm{BSSE}}(\mathrm{THF}\cdot\mathrm{Et_3Al})$. Here, $(\sim xy)$·3THF is considered as a single molecule for which $\bar{E}_{\mathrm{BSSE}} = 0$. Taking the data in Table 3, this gives at the B3LYP/TZVP//BP86/SVP level of theory, $\Delta E_{mm}(7) = -8.7$ kJ/mol, $\Delta E_{mr}(7) = -24.4$ kJ/

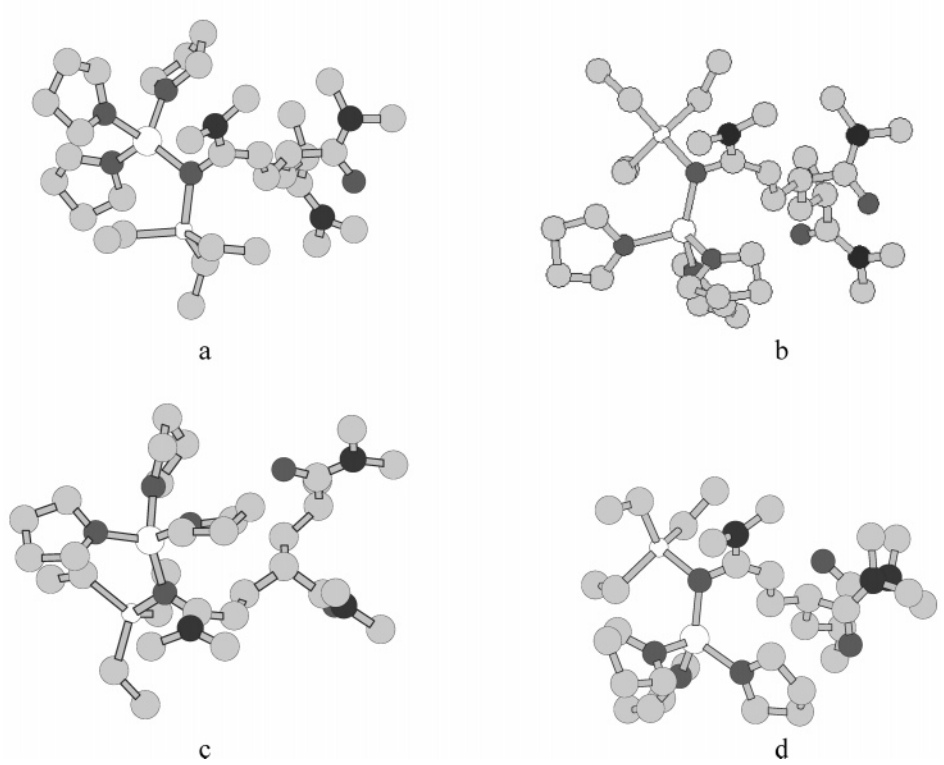

Figure 5. DFT-optimized structures of *mm*-triad·3THF·Et_3Al (a), *mr*-triad·3THF·Et_3Al (b), *rm*-triad·3THF·Et_3Al (c), and *rr*-triad·3THF·Et_3Al (d). Aluminum atoms are shown as smaller white spheres. Other atoms are shown in the same way as in Figure 1.

Scheme 4. Competing Interactions of Et_3Al and DFT-Calculated Energy Differences

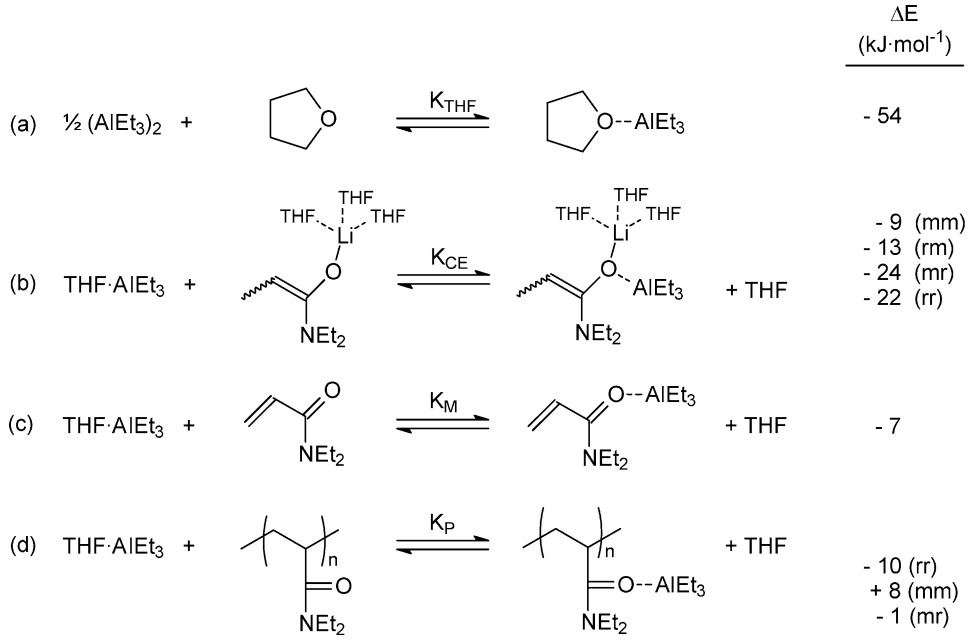

mol, $\Delta E_{rm}(7) = -13.3$ kJ/mol, and $\Delta E_{rr}(7) = -21.9$ kJ/mol. An averaged estimation $\Delta E_{xy}(7) \approx -17$ kJ/mol is not so much negative for the equilibrium (7) to be shifted to the right completely at low [Et_3Al].

It is seen from Table 3 that in the presence of Et_3Al the $(\sim mm)_1$·3THF·LA structure (Figure 5a, bond angle C−O−Li ≅ 115°) is 15 kJ/mol less stable than $(\sim mr)_1$·3THF·LA (Figure 5b, bond angle C−O−Li ≅ 117°) and the $(\sim rm)_1$·3THF·LA structure (Figure 5c, bond angle C−O−Li ≅ 118°) is ca. 10 kJ/mol less stable than $(\sim rr)_1$·3THF·LA (Figure 5d, bond angle C−O−Li ≅ 120°). These data show that nearly only the prochiral terminal *r*-dyad is formed on the complexation of chain ends with Et_3Al.

To become active in propagation, a dormant LA-complexed chain end should first lose Et_3Al. Comparing the BSSE-corrected values $\Delta E_{mr}(7) = -24.4$ kJ/mol and $\Delta E_{rr}(7) = -21.9$ kJ/mol, one may conclude that there is somewhat less LA-free (i.e., reactive) $\sim mx$ units, and the polymerization proceeds more through LA-free $\sim rx$ units. However, (a) the energy difference is not large enough to allow for only $\sim rx$ units to propagate, and (b) there will be monomer additions in both *m* and *r* fashion, leading to a predominant heterotactic structure of resulting

polymer chains in a satisfactory agreement with the experimental data.[16,17,21,22]

Conclusions

Four species compete for binding to Et_3Al: THF, chain ends, and monomer and polymer amide groups, the position of the respective equilibria depending on their relative energies and concentrations. In addition, the LA-complexed chain ends are less active than the uncomplexed ones, whereas complexation of LA with monomer leads to its activation. This makes it possible to explain the dependences of the apparent polymerization rate constant on the concentration of monomer and Et_3Al.[21,22] The most important energy differences are listed in Scheme 4.

The addition of Et_3Al induces the deaggregation of the dimeric associates of the monomeric model compound DMPA-Li. However, the trimer models of the PDMAAm-Li chain ends appear to be mostly nonassociated at the relevant concentrations in the mmol/L range.

To explain the decrease of polymerization rate with [Et_3Al], we must assume that there is a dynamic equilibrium between LA-complexed and LA-free chain ends, only the latter ones contributing to propagation. As follows from the data of Table 3, complexations of both $(\sim mx)_1$·3THF and $(\sim rx)_1$·3THF chain ends with Et_3Al produce LA-complexed chain ends with preferably *r* terminal dyad. As the complexation process is slightly more exothermic for $(\sim mx)_1$·3THF ($\Delta E_{mr}(7) = -24.4$ kJ/mol) than for $(\sim rx)_1$·3THF ($\Delta E_{rr}(7) = -21.9$ kJ/mol), there should be somewhat less LA-free (i.e., reactive) $\sim mx$ units, and the polymerization proceeds to a higher extent through LA-free $\sim rx$ units. However, the energy difference is not too large to exclude the participation of $\sim mx$ units in propagation, leading to the observed heterotactic structure of resulting polymers.[16,17,21,22]

Acknowledgment. A.V.Y. is grateful to Deutsche Forschungsgemeinschaft for financial support.

Supporting Information Available: Calculated absolute total energy values, *E* (in hartrees), the BP86/SVP-optimized Cartesian coordinates (in Å), and input files for visualization with the HYPERCHEM software (extension.hin) for all structures presented in Figures 1−5. This material is available free of charge via the Internet at http://pubs.acs.org.

References and Notes

(1) Wang, Y.; Hu, S.; Li, H.; Allbritton, N. L.; Sims, C. E. *J. Chromatogr., A* **2003**, *1004*, 61−70.
(2) Albarghouthi, M. N.; Buchholz, B. A.; Doherty, E. A. S.; Bogdan, F. M.; Zhou, H.; Barron, A. E. *Electrophoresis* **2001**, *22*, 737−747.
(3) Ren, J.; Ulvik, A.; Refsum, H.; Ueland, P. M. *Anal. Biochem.* **1999**, *276*, 188−194.
(4) Hirose, M.; Kwon, O. H.; Yamato, M.; Kikuchi, A.; Okano, T. *Biomacromolecules* **2000**, *1*, 377−381.
(5) Aoki, T.; Kawashima, M.; Katono, H.; Sanui, K.; Ogata, N.; Okano, T.; Sakurai, Y. *Macromolecules* **1994**, *27*, 947−952.
(6) Sawada, H.; Iidzuka, J.-i.; Maekawa, T.; Takahashi, R.; Kawase, T.; Oharu, K.; Nakagawa, H.; Ohira, K. *J. Colloid Interface Sci.* **2003**, *263*, 1−3.
(7) McCormick, C. L.; Elliott, D. L. *Macromolecules* **1986**, *19*, 542−547.
(8) Butler, K.; Thomas, P. R.; Tyler, G. J. *J. Polym. Sci.* **1960**, *48*, 357−366.
(9) Nakhmanovich, B. I.; Urman, Y. G.; Arest-Yakubovich, A. A. *Macromol. Chem. Phys.* **2001**, *202*, 1327−1330.
(10) Kobayashi, M.; Ishizone, T.; Nakahama, S. *Macromolecules* **2000**, *33*, 4411−4416.
(11) Kobayashi, M.; Okuyama, S.; Ishizone, T.; Nakahama, S. *Macromolecules* **1999**, *32*, 6466−6477.
(12) Ishizone, T.; Yoshimura, K.; Hirao, A.; Nakahama, S. *Macromolecules* **1998**, *31*, 8706−8712.
(13) Xie, X.; Hogen-Esch, T. E. *Macromolecules* **1996**, *29*, 1746−1752.
(14) Nakahama, S. K. M.; Ishizone, T.; Hirao, A. *J. Macromol. Sci., Pure Appl. Chem.* **1997**, *A34*, 1845−1855.
(15) Kobayashi, M.; Ishizone, T.; Hirao, A.; Nakahama, S. *Polym. Mater. Sci. Eng.* **1997**, *76*, 304−305.
(16) Nakhmanovich, B. I.; Urman, Y. G.; Krystal'nyi, E. V.; Arest-Yakubovich, A. A. *Vysokomol. Soedin., Ser. A Ser. B* **2003**, *45*, 978−981.
(17) Martinez-Castro, N.; Müller, A. H. E. *Des. Monomers Polym.*, in press.
(18) Park, T. G.; Hoffman, A. S. *J. Appl. Polym. Sci.* **1992**, *46*, 659−671.
(19) Freitag, R.; Baltes, T.; Eggert, M. *J. Polym. Sci., Part A: Polym. Chem.* **1994**, *32*, 3019−3030.
(20) André, X.; Müller, A. H. E. *Macromol. Rapid Commun.* **2005**, *26*, 558−563.
(21) André, X.; Benmohamed, K.; Yakimansky, A. V.; Litvinenko, G. I.; Müller, A. H. E. *Macromolecules*, published on the internet on March 28, 2006.
(22) André, X.; Benmohamed, K.; Yakimansky, A. V.; Müller, A. H. E. *Proceedings of the 40th IUPAC International Symposium on Macromolecules (MACRO 2004)*, 2004; http://www.e-Polym..org/paris/data/L4065.pdf.
(23) Häser, M.; Ahlrichs, R.; Baron, H. P.; Weis, P.; Horn, H. *Theor. Chim. Acta* **1992**, *83*, 455−470.
(24) Becke, A. D. *Phys. Rev. A* **1988**, *38*, 3098−3100.
(25) Perdew, J. P.; Levy, M. *Phys. Rev. B* **1986**, *33*, 8822−8824.
(26) Vosko, S. H.; Wilk, L.; Nusair, M. *Can. J. Phys.* **1980**, *58*, 1200−1211.
(27) Vahtras, O.; Almloef, J.; Feyereisen, M. W. *Chem. Phys. Lett.* **1993**, *213*, 514−518.
(28) Eichkorn, K.; Treutler, O.; Oehm, H.; Häser, M.; Ahlrichs, R. *Chem. Phys. Lett.* **1995**, *242*, 652−660.
(29) Eichkorn, K.; Weigend, F.; Treutler, O.; Ahlrichs, R. *Theor. Chem. Acc.* **1997**, *97*, 119−124.
(30) Becke, A. D. *J. Chem. Phys.* **1993**, *98*, 5648−5652.
(31) Lee, C.; Yang, W.; Parr, R. G. *Phys. Rev. B: Condens. Matter Mater. Phys.* **1988**, *37*, 785−789.
(32) Treutler, O.; Ahlrichs, R. *J. Chem. Phys.* **1995**, *102*, 346−354.
(33) Eichkorn, K.; Treutler, O.; Oehm, H.; Haeser, M.; Ahlrichs, R. *Chem. Phys. Lett.* **1995**, *240*, 283−290.
(34) Schäfer, A.; Horn, H.; Ahlrichs, R. *J. Chem. Phys.* **1992**, *97*, 2571−2577.
(35) Ditchfield, R. *Mol. Phys.* **1974**, *27*, 789−807.
(36) Schäfer, A.; Huber, C.; Ahlrichs, R. *J. Chem. Phys.* **1994**, *100*, 5829−5835.
(37) TURBOMOLE on the Internet: http:/www.chemie.uni-karlsruhe.de/PC/TheoChem/, ftp://ftp.chemie.uni-karlsruhe.de.pub.
(38) Boys, S. B.; Bernardi, F. *J. Mol. Phys.* **1970**, *19*, 553.
(39) Salvador, P.; Paizs, B.; Duran, M.; Suhai, S. *J. Comput. Chem.* **2001**, *22*, 765−786.
(40) Yakimansky, A. V.; Müller, A. H. E. *Macromolecules* **1999**, *32*, 1731−1736.
(41) Yakimansky, A. V.; Müller, A. H. E.; Van Beylen, M. *Macromolecules* **2000**, *33*, 5686−5692.
(42) Yakimansky, A. V.; Müller, A. H. E. *J. Am. Chem. Soc.* **2001**, *123*, 4932−4937.
(43) Weigend, F.; Haser, M.; Patzelt, H.; Ahlrichs, R. *Chem. Phys. Lett.* **1998**, *294*, 143−152.
(44) Champagne, B.; Mosley, D. H.; Fripiat, J. G.; André, J.-M.; Bernard, A.; Bettonville, S.; Francois, P.; Momtaz, A. *THEOCHEM* **1998**, *454*, 149−159.
(45) Baskaran, D. *Prog. Polym. Sci.* **2003**, *28*, 521−581.
(46) Schmitt, B.; Schlaad, H.; Müller, A. H. E.; Mathiasch, B.; Steiger, S.; Weiss, H. *Macromolecules* **1999**, *32*, 8340−8349.
(47) Frère, Y.; Gramain, P. *Macromolecules* **1992**, *25*, 3184−3189.
(48) Müller, A. H. E.; Hogen-Esch, T. E. *Macromolecules* **1988**, *21*, 2336−2339.

MA060385R